Updates to the traceability of mm-wave power measurements at NIST

Aaron M. Hagerstrom*, Angela C. Stelson*, Jeffrey A. Jargon*, Christian J. Long*
*National Institute of Standards and Technology

***Abstract*—Metrological traceability helps ensure the reliability of measurements by allowing them to be compared with established international standards with well-understood uncertainties. A thorough uncertainty analysis is therefore necessary to provide traceable measurements. In this paper, we summarize recent updates to the measurement procedures and uncertainty analysis for NIST's calibrations of power sensors with WR-15 connectors. The improvements include a more detailed uncertainty analysis with a more complete treatment of type A uncertainty, and the establishment of traceability of DC voltage measurements and scattering parameter measurements to primary standards.**

***Index Terms*—Traceability, mm-wave power measurements**

I. Introduction

Microwave and mm-wave power measurements are fundamental in communications metrology. Power measurements support more complex measurements, including wave parameters, noise, and antenna gain. By definition, traceable measurements can be compared to references (ultimately, the definitions of the SI units) with uncertainty estimates at every step. Thus, a rigorous uncertainty analysis is a key part of any claim of traceability.

One of the ways NIST verifies its measurements and uncertainties is by participating in international key comparisons, where travelling standards are measured by different National Metrology Institutes around the world. At the time of writing in 2021, an international intercomparison is currently underway to compare WR-15 calorimetric power calibrations. WR-15 waveguides operate in a frequency band of 50 GHz to 75 GHz. This paper describes updates to the measurement procedures and uncertainty analysis made in advance of the key comparison to strengthen the traceability of these measurements.

Traditionally, NIST's traceable mm-wave power measurements have been based around the concept of DC substitution [1]. This technique relies on sensors with temperature-dependent resistors (either negative-temperature-coefficient thermistors or platinum thin-films) which can be heated by either DC or microwave power. During a DC substitution measurement, a DC bias voltage is applied to the thermistor. This bias voltage is supplied by a feedback loop configured to maintain the thermistor at a constant resistance. When an external mm-wave power is applied, the feedback loop decreases the applied DC voltage to keep the resistance constant, and by extension, keep the dissipated power *approximately* constant. Thus, microwave power traceability is achieved by comparing microwave power to DC power. DC voltage and current sensors can be very accurately and traceably calibrated in comparison with microwave and mm-wave power sensors.

However, microwave and DC power are not exactly equivalent because microwave power can be absorbed in other parts of the sensor besides the thermistor, among other factors [1]. Their non-equivalence is characterized by the effective efficiency, η, which relates the absorbed power by a sensor to the DC-substituted power. Thus, η features prominently in NIST's approach to microwave power traceability. For this reason, NIST offers effective efficiency measurements to external customers as a measurement service. The most accurate effective efficiency measurements are provided by an instrument called a calorimeter or microcalorimeter [1].

Roughly speaking, a calorimeteric measurement characterizes a power sensor by measuring heating caused by electrical power (both microwave and DC) dissipated in a sensor. This power measurement is then compared with the DC substituted power to calculate effective efficiency. However, there is a systematic error that must be corrected to achieve accurate measurements. In addition to the sensor, microwave power is also dissipated in the waveguide leading up to the sensor [2]. The amount of dissipated power depends on the standing waves in the waveguide, and therefore depends on the reflection coefficient of the sensor, Γ_M. The size of the correction is parameterized by a dimensionless number called the "intrinsic correction factor" (denoted g_c). Taking the correction into account, the effective efficiency is given by:

$$\eta = \left[1 + g_c \left(\frac{1 + |\Gamma_M|^2}{1 - |\Gamma_M|^2}\right)\right] \eta^{(\text{unc})}, \tag{1}$$

where $\eta^{(\text{unc})}$ is uncorrected effective efficiency [3].

Our discussion of the uncertainty analysis is organized by the three quantities appearing in Equation (1). These three quantities, $\eta^{(\text{unc})}$, Γ, and g_c, are measured in separate experiments, and so we discuss their traceability separately in Sections II, III, and IV respectively.

Our approach to traceability is based on Reference [3], which introduced an approach that uses a Vector Network Analyzer (VNA) to measure g_c and allows for correlated uncertainty propagation. Tracking frequency correlations in uncertainties is important because these correlations can have a large impact on modulated signal measurements [4].

The current paper extends the work reported in Reference [3] in two major respects. First, we include a much more extensive uncertainty analysis, which includes repeated measurements of $\eta^{(\text{unc})}$, and a more extensive analysis of both type A and type B uncertainty mechanisms affecting Γ_M. The second major way in which this work differs from Reference [3] is that while that paper outlined an approach to traceable measurements, the scattering parameter and voltage measurements were not traceable to primary standards. Since the publication of Reference [3], scattering parameter meaurements traceable to NIST's dimensional metrology service,

and voltage calibrations traceable to primary standards have become available.

II. Uncorrected effective efficiency, $\eta^{(\mathrm{unc})}$

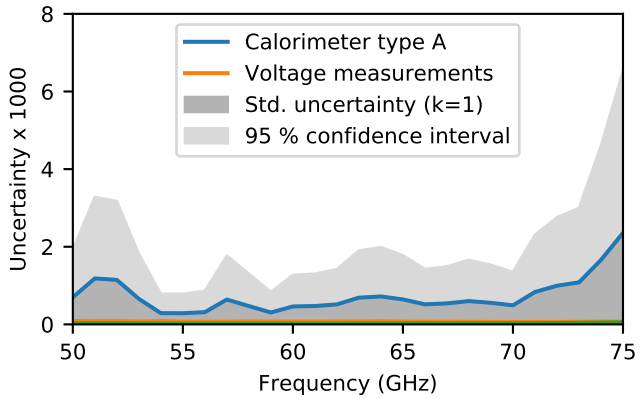

Fig. 1: The uncertainty budget for $\eta^{(\mathrm{unc})}$ of a particular sensor (15P3). The standard uncertainties associated with the two largest uncertainty mechanisms are shown. The type A uncertainty is large enough compared to the other contributions that it can't be distinguished from the total uncertainty visually. Also note that the 95 % confidence interval is more than twice as large as the $k = 1$ standard uncertainty because of the finite number of degrees of freedom.

The uncorrected effective efficiency, $\eta^{(\mathrm{unc})}$, is measured in a calorimeter. NIST's WR-15 calorimeter employs a twin-load design [5]. The twin-load design has two thermally identical sensors. One of these sensors is the device under test (DUT), while the other is a dummy. The DUT is heated by both DC and mm-wave power, while the dummy is not. This dissipated power generates a temperature difference between the sensors. To measure the temperature difference, and therefore the dissipated power, a thermopile is placed between the sensors. The thermopile voltage, e is related to the dissipated power by:

$$E = \frac{V^2}{R} + \left[1 + g_c \left(\frac{1+|\Gamma_M|^2}{1-|\Gamma_M|^2}\right)\right] P_{mw} \quad (2)$$

$$E \equiv k_1 e + k_2 e^2, \quad (3)$$

where V is the DC bias voltage supplied to the sensor, R is the resistance of the thermistor (nominally 200 Ω), P_{mw} is microwave power, and k_1 and k_2 are constants describing the thermopile nonlinearity.

Note that the model given here differs from [3] in its description of the thermopile nonlinearity. The form here is reliable over a wider range of input power. To measure k_1 and k_2, we attached a special standard in place of the sensor. This standard consists of a quarter-wave offset short that is designed to have the same thermal characteristics as a sensor, and contains a 200 Ω fixed resistor so that the standard can be heated by applying DC power [2]. With this standard attached, we applied a range of bias voltages, and measured the thermopile voltage. This procedure was repeated several times to estimate the uncertainty due to mechanical repeatability. The uncertainty in k_1 and k_2 due to DC voltage and current measurements was negligible.

To determine $\eta^{(\mathrm{unc})}$, we perform voltage measurements in two states: with microwave power applied (denoted "on"), and with no microwave power applied ("off"). In terms of these measurements, the uncorrected effective efficiency is given by:

$$\eta^{(\mathrm{unc})} = \frac{1 - (V_{\mathrm{on}}/V_{\mathrm{off}})^2}{E_{\mathrm{on}}/E_{\mathrm{off}} + (V_{\mathrm{on}}/V_{\mathrm{off}})^2} \quad (4)$$

We see that $\eta^{(\mathrm{unc})}$ is a unitless quantity, and therefore can't be directly compared to the definitions of the SI base units. Likewise, the voltage measurements that are used to compute $\eta^{(\mathrm{unc})}$ enter into the equation as unitless ratios. Even though voltages enter the equation as ratios, any offsets or noise in the voltage measurements contribute to the measurement uncertainty in the uncorrected effective efficiency. Therefore, it is important to implement traceable voltage measurements as part of the traceability path for effective efficiency.

Figure 1 summarizes the uncertainty contributions that affect $\eta^{(\mathrm{unc})}$. The uncertainty is dominated by the connect-disconnect uncertainty ("Calorimeter type A"). This mechanism was assessed from 5 recent measurements. In order to allow for correlated uncertainty propagation, we constructed the sample covariance matrix from the measurements (treated as vectors where each index is a real-valued measurand at a frequency point), performed and eigenvalue decomposition, and treated each eigenvector as an independent uncertainty mechanism. At a single point, this approach yields identical results to the typical approach of computing the standard deviation of repeated measurements. However, the approach here has the advantage of modeling covariance between frequency points.

The uncertainties arising from voltage measurements were also evaluated ("Voltage" in Figure 1). The thermopile voltages e_{on} and e_{off} are relatively important in the uncertainty analysis. The nanovoltmeter, which measures the thermopile voltage, is calibrated by the Sources and Detectors Group at NIST. This calibration is performed using a multimeter calibrated with a NIST-traceable 10 V voltage artifact (NIST Service ID 53160C) and NIST-traceable 10 kΩ resistance artifact (NIST Service ID 51140C). The calibration validates the manufacturer's specifications, and the manufacturer's uncertainty model was used here. Uncertainties in the sensor bias voltage (V_{on} and V_{off}) are not an important contribution to the overall uncertainty (line C). The voltmeter that was used to perform these bias measurements was verified by comparison to a calibrated nanovoltmeter.

III. Scattering parameters

One of the major upgrades to the traceability of calorimetry was the implementation of traceable Scattering (S-) parameter measurements performed on a vector network analyzer (VNA). As with $\eta^{(\mathrm{unc})}$, S-parameters are unitless quantities. Therefore, to establish traceability, we ensure that the measurements involved in the uncertainty evaluation are traceable. The measurement uncertainties arise from a variety of sources, as

enumerated in Reference [6]: characterization of calibration standards, noise floor and trace noise, VNA non-linearity, VNA drift, isolation (cross-talk), test port cable stability, and connection repeatability.

The characterization of calibration standards deserves special attention, as it contributes a large fraction of the overall uncertainties, and because they can be directly traced back to more fundamental measurements. In the measurements reported here, we employed a Short-Open-Load (SOL) calibration. The definitions of the SOL standards are derived from measurements performed on a VNA calibrated by a Multiline-Thru-Reflect-Line (MTRL) calibration [7]. Some of the most important parameters in an MTRL calibration are the mechanical dimensions of the standards. These mechanical dimensions were measured traceably by the NIST Dimensional Metrology group (NIST Service ID 11050S), and we recently undertook a detailed analysis of their effects on the uncertainties of our measurements [8].

We also evaluated other instrumentation-related uncertainty mechanisms by a type A approach. In other words, these uncertainties were estimated from repeated measurements, very similar to those described in [6]. A full account of these measurements is beyond the scope of this paper. In the analysis presented here, several uncertainty mechanisms are omitted. Noise floor, trace noise, and isolation are omitted because they were found to have a negligible effect compared to other mechanisms effecting the S-parameters. The VNA non-linearity is omitted because our analysis is not complete at the time of writing. However, we estimate that this uncertainty mechanism will also have a minimal effect on the overall uncertainty of effective efficiency. On the other hand, connection repeatability, test port cable stability, and VNA drift were implemented.

IV. Intrinsic correction factor, g_c

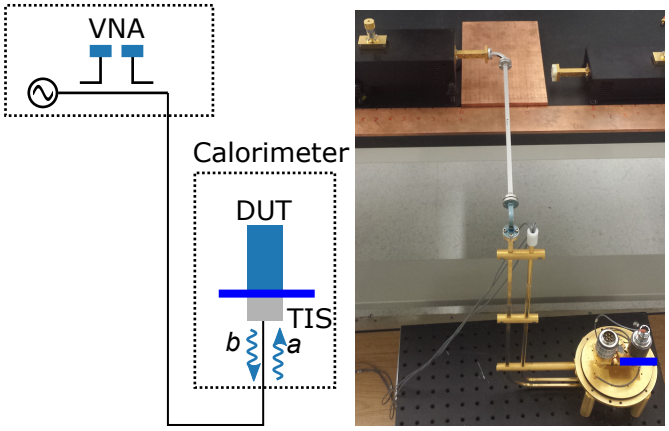

Fig. 2: Experimental setup. The waveguide immediately before the sensor is called the thermal isolation section (TIS). The goal of the g_c measurement is to characterize microwave loss in this section.

Figure 2 shows our approach to measuring g_c (based on [3]). Recall that the goal of measuring g_c is to correct for power dissipated in the waveguide leading up to the sensor ("DUT"). The experimental procedure involves measurements quite similar to a normal calorimetric measurement as described in Section II, except that the power sensor is replaced with the same special offset short standard (described in Reference [2]) that was used in the thermopile nonlinearity measurement. Since the special standard absorbs a minimal amount of microwave power, microwave power measured by the thermopile can be mostly attributed to power absorbed in the waveguide.

To measure the power incident on the special standard, we use a VNA. First, an SOL calibration is performed at the reference plane inside the calorimeter, where the sensor is normally attached. Then, to calibrate the power, a sensor is placed in the calorimeter, and the DC-substituted power is measured. Finally, the sensor is replaced by the special standard, and the thermopile voltage is recorded with microwave power applied, and with no microwave power applied.

To determine g_c, we assume that both the measurements with the special standard, and the measurements with the power sensor are both consistent with Equations (2 and 3). This leads to Equations (5-8).

$$g_c = \frac{-\left(1-|\Gamma_S|^2\right)A + \eta^{(\mathrm{unc})}B}{\left(1+|\Gamma_S|^2\right)A - MB} \tag{5}$$

$$M \equiv \frac{1+|\Gamma_M|^2}{1-|\Gamma_M|^2} \tag{6}$$

$$A \equiv \frac{|a_S|^2}{E_{\mathrm{on}} - E_{\mathrm{off}}} \tag{7}$$

$$B \equiv \frac{R|a_M|^2}{V_{\mathrm{off}}^2 - V_{\mathrm{on}}^2} \tag{8}$$

Here, the subscript M refers to measurements with a sensor, S refers to measurements with the special reflect, and "on" and "off" refer to measurements with and without microwave power applied.

Figure 3 shows the major uncertainty mechanisms affecting g_c. The repeatability of the measurements was assessed by measuring g_c twice with different sensors. The difference between these two measurements is denoted "gc repeatability". This uncertainty mechanism primarily reflects the mechanical repeatability of the waveguide connections in the measurement setup. At about half of the frequencies tested, gc repeatability was the largest contribution to the uncertainty of g_c.

The second most important uncertainty mechanism is the type A uncertainty of the S-parameters. This category includes the disconnect-reconnect uncertainty of the SOL standards (measured during their characterization), the cable stability, and the VNA drift. Counterintuitively, the type A uncertainties are a much larger contribution than the type B uncertainties, even though the type B uncertainties are larger in most S-parameter measurements.

The S-parameter contribution to the uncertainties in g_c is dominated by the $(1-|\Gamma_S|^2)$ term in Equation 5. The physical models of the calibration standards described in Reference [8] have very little energy loss. When these models are applied

to a nearly lossless device (like the special standard), they predict very little uncertainty in the magnitude of the reflection coefficient. On the other hand, the type A analysis accounts for factors like drift and cable movement which can change the magnitude of the measured reflection coefficient even if no energy is absorbed in the special standard.

Figure 3 also compares the measurements reported here to Reference [3]. The measurement in Reference [3] is well within the 95 % confidence interval. Our analyses also agree on the leading uncertainty mechanism (other than g_c repeatability, which [3] did not assess). Both analyses concluded that the type A uncertainties of the reflection coefficient of the special reflect standard was a leading source of uncertainty. While the conclusions are the same, the algorithms and procedures that were employed to assess the type A uncertainties were quite different. Reference [3] derives the type A uncertainties from repeated measurements of the special reflect standard, while we derive type A uncertainties from models that were built from other experiments. Our conclusions are robust to these changes in methodology.

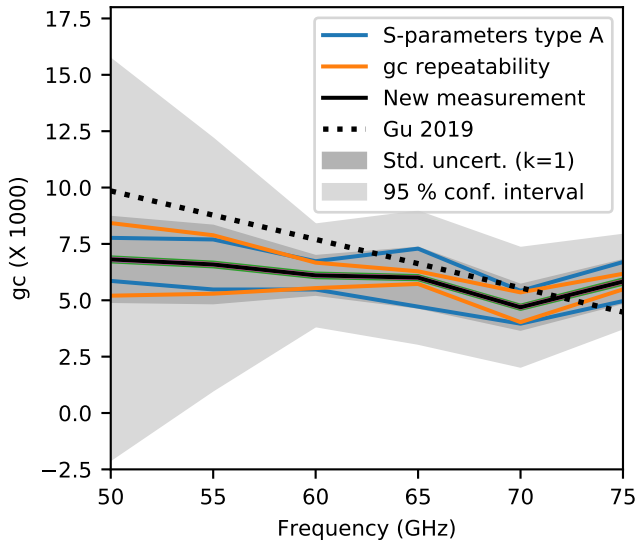

Fig. 3: The measured value of g_c with uncertainties (both $k = 1$ and 95 % confidence interval), and the standard uncertainty contributions of the largest two uncertainty mechanisms. The previous measurement of g_c is shown for comparison. Note that Reference [3] modeled g_c as having a linear frequency dependence.

V. Summary

Figure 4 summarizes the major uncertainty contributions to the effective efficiency. As we saw in Figure 1, the connect-disconnect uncertainty of the sensor was the largest contribution to the uncorrected effective efficiency $\eta^{(\mathrm{unc})}$. Likewise, it is a large contribution to the corrected η. The other major contributions come from g_c, and are seen in Figure 3. While it would appear that the type B uncertainties in the scattering parameters are a small contribution, they are still important to power traceability. In addition to effective efficiency, power

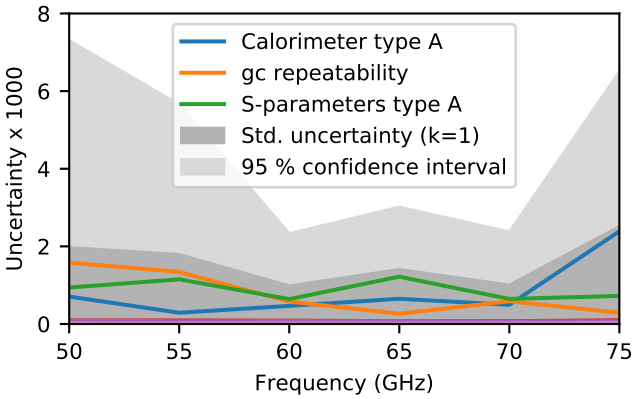

Fig. 4: Overall uncertainty budget (both $k = 1$ and 95 % confidence interval) for the effective efficiency of a particular senor. The standard uncertainty contributions of the three largest uncertainty mechanisms are shown. These contributions account for most of the uncertainty.

calibrations are often reported in terms of the calibration factor, $K = \left(1 - |\Gamma_M|^2\right)\eta$, which relates power incident on a sensor to the DC substituted power. This quantity is more sensitive to Γ_M, and to the type B mechanisms.

In conclusion, we have established rigorous traceability for WR-15 calorimetric power measurements. This effort includes establishing traceability to primary standards for the voltage measurements, and for the scattering parameter measurements involved in calorimetry. Additionally, we have incorporated an extensive type A uncertainty on both the calorimetric measurements and the scattering parameter measurements that support them. Every part of this analysis employs correlated uncertainty propagation.

References

[1] J. W. Allen, F. R. Clague, N. T. Larsen, and M. P. Weidman, "The nist microwave power standards in waveguide," 1999.

[2] X. Cui and T. P. Crowley, "Comparison of experimental techniques for evaluating the correction factor of a rectangular waveguide microcalorimeter," *IEEE Transactions on Instrumentation and Measurement*, vol. 60, no. 7, pp. 2690–2695, 2011.

[3] D. Gu, X. Lu, B. F. Jamroz, D. F. Williams, X. Cui, and A. W. Sanders, "Nist-traceable microwave power measurement in a waveguide calorimeter with correlated uncertainties," *IEEE Transactions on Instrumentation and Measurement*, vol. 68, no. 6, pp. 2280–2287, 2019.

[4] K. A. Remley, D. F. Williams, P. D. Hale, C. Wang, J. Jargon, and Y. Park, "Millimeter-wave modulated-signal and error-vector-magnitude measurement with uncertainty," *IEEE Transactions on Microwave Theory and Techniques*, vol. 63, no. 5, pp. 1710–1720, 2015.

[5] T. P. Crowley and Xiaohai Cui, "Design and evaluation of a wr-15 (50 to 75 ghz) microcalorimeter," in *2008 Conference on Precision Electromagnetic Measurements Digest*, 2008, pp. 420–421.

[6] M. Zeier, D. Allal, and R. Judaschke, "Euramet calibration guide no. 12: Guidelines on the evaluation of vector network analysers (vna)," *European Association of National Metrology Institutes, Braunschweig*, vol. 3.

[7] R. B. Marks, "A multiline method of network analyzer calibration," *IEEE transactions on microwave theory and techniques*, vol. 39, no. 7, pp. 1205–1215, 1991.

[8] J. A. Jargon, D. F. Williams, A. C. Stelson, C. J. Long, A. M. Hagerstrom, P. D. Hale, J. R. Stoup, E. S. Stanfield, and W. Ren, "Physical models and dimensional traceability of wr15 rectangular waveguide standards for determining systematic uncertainties of calibrated scattering-parameters," 2020.